Korean J. Chem. Eng., 37(7), 1251-1257 (2020)
DOI: 10.1007/s11814-020-0519-0

pISSN: 0256-1115
eISSN: 1975-7220

Synthesis of size-controlled Ag nanowires via a seed-mediated growth method

Kwang-Hun Jeon and Seog-Jin Jeon†

Department of Polymer Science and Engineering, Kumoh National Institute of Technology, Gumi, Gyeongbuk 39177, Korea
(*Received 30 December 2019 • Revised 29 January 2020 • Accepted 19 February 2020*)

Abstract−Seed-mediated growth has attracted much attention due to the wide range of controllability in size and shape, improved reproducibility, and capability to form bimetallic structures. Especially, seed-mediated growth of Ag has been extensively studied due to the excellent electrical, thermal, optical, and catalytic properties of Ag, but it has been conducted mainly for isotropic seeds such as nanocubes, and relatively little attention has been given to anisotropic seeds such as nanowires. We studied the seed-mediated growth of Ag nanowires for their size control, exploring the effect of hydrochloric acid (HCl), capping agents, and seeds to find the experimental condition for heterogeneous nucleation. By the optimized condition, the length and diameter were grown up to nearly 7 and 12 times, respectively, by those of seeds. Interestingly, for the condition that causes homogeneous nucleation, Ag particles of various shapes, including nanocubes, nanowires, and micro rods, were synthesized. The size-controlled Ag nanowires and Ag particles of various shapes obtained in this work are expected to be applied for the study of low resistance electrodes and the size- and shape-dependent properties of metal nanomaterials.

Keywords: Size-controlled, Ag Nanowires, Seed-mediated Growth, Various Shapes

INTRODUCTION

Seed mediated growth of noble metal nanomaterials has attracted much attention due to the wide range of controllability in size and shape, improved reproducibility, and capability to form bimetallic structures [1,2]. The key to success with seed-mediated growth is to inhibit homogeneous nucleation, the process of creating new seeds, and to induce heterogeneous nucleation in which already generated seeds grow. LaMer and Dinegar explained that homogeneous nucleation is dominant when the precursor is supersaturated, and heterogeneous nucleation is predominant when precursor concentration lowers than the critical concentration by consumption of precursors [3]. Therefore, the success of seed growth lies in efficient precursor growth on the seed surface with the precursor concentration below the critical concentration.

In particular, seed-mediated growth of Ag has been widely studied due to its high electrical conductivity [4,5], unique optical and catalytic property of Ag [6-9], and a large variety of controllable shapes in *Nanoscale* at a relatively low cost [10-12]. For the development of seed-mediated growth, accumulated knowledge from extensive work on one-pot synthesis of Ag for several decades has greatly helped in understanding seed-mediated growth [13-23]. The successful seed-mediated growth begins with the selection of the appropriate capping agents and additives. A capping agent biased to the specific crystal facet of Ag determines the structure of final products [13]. For example, PVP that binds more strongly to Ag (100) selectively stabilizes such facets, and thus causes cubes [14]. PVP also plays a vital role as a reducing agent, so the optimization of its concentration is critical [15-17]. As an additive, it has been reported that the use of HCl [18], Cl^- [19-21], Fe(II) [22], and Cu(I) [23] greatly influenced the shape and uniformity of the final products even in very small quantities. For example, the change in surface energy of Ag facets caused by the Cl^- concentration results in the formation of Ag nanocubes [21]. And the role played by Fe(II) or Cu(I) is to prevent the growth of nanowires to Ag {100} facets, which causes long nanowires with small diameters [19-23].

Seed-mediated growth of Ag has been conducted for the control of both size and shape, but the shape of the seeds was mainly Ag nanocubes [14,24-27]. For example, Ag nanocubes have been grown up to several micrometers [26], and monodisperse Ag nanospheres have been obtained from nanocubes by seed-mediated growth followed by oxidative etching [27]. While systematic research has been conducted on nanocubes, only fractional results are known for seeds other than nanocubes. For example, there are only a few studies on the seed-mediated growth of Ag nanowires [4,5,28,29], and they are mostly towards obtaining high aspect ratio nanowires for their use as transparent electrodes. Lee et al. and Zhang et al. fabricated high aspect ratio nanowires by multistep growth by utilizing controlled sonication and seeds screening, respectively [4,5]. There also have been a number of studies for the preparation of high aspect ratio nanowires or nanorods by seed-mediated growth, though decahedron seeds were used [6-9]. The strategy of obtaining high aspect ratio nanowires is to grow only the length while suppressing the growth of the thickness. But the control of the thickness of nanowires is also important in a specific application. For example, Wiley et al. reported that the thickening of Ag nanowires helps improve the performance of the transparent electrode in case of low sheet resistance application [30]. And the thickening of Ag nanowires is known to affect their mechanical properties [31-35]. But the control of the thickness of Ag nanowires has been largely unexplored.

In this study, we describe nucleation routes of the seed-mediated

†To whom correspondence should be addressed.
E-mail: sjjeon@kumoh.ac.kr
Copyright by The Korean Institute of Chemical Engineers.

growth of Ag nanowires and regarding products. Seed-grown nanowires were successfully obtained by heterogeneous nucleation, and their size was statistically analyzed to provide a controllable size range of Ag nanowires by this approach. We show that the seed-mediated growth exhibits fast growth in thickness than length, which causes reduced aspect ratio. We also discuss the products obtained by homogeneous nucleation, i.e., nanocubes. The way to control the thickness of nanowires will open new possibilities to enhance electrical conductivity for low sheet resistance electrodes[30] and enable study about the size-dependent properties of metals in the region between nano- to micro-meters [31-38].

MATERIALS AND METHODS

1. Materials

Ethylene glycol (EG, Merck), hydrochloric acid (HCl, 37%, Daejung), copper(II) chloride ($CuCl_2$, Aldrich) Ag nitrate ($AgNO_3$, ≥99.0%, Aldrich), polyvinylpyrrolidone (PVP 55k, MW=55,000 g/mol, Aldrich), and polyvinylpyrrolidone (PVP 360k, MW=360,000 g/mol, Aldrich) were used as received. A 22 mL vial (Agilent) and Teflon coated spin bar (15.9 mm×6.4 mm) were used. High purity grade argon (99.999%) was purchased from Singin Gastech.

2. Synthesis of Seed Nanowires

We followed the procedure of Korte et al. for the synthesis of seed nanowires [23]. Typically, 5 mL of EG was preheated at 151.5 °C for 1 hour with stirring (280 rpm) in a 22 mL vial, and 40 μL of 4 mM $CuCl_2$ solution in EG was added into the vial. After 15 min, 1.5 mL of 0.14 M PVP in EG was injected. The concentration of PVP is based on the molecular weight of the repeating unit of PVP (111.1 g/mol). After 2 min, 1.5 mL of 0.094 M $AgNO_3$ in EG was added with the injection rate of 150 μL/min to prevent supersaturation of Ag atoms. After 1 hour, the product was quenched in a water bath at room temperature. It was washed with acetone once and with water several times to remove EG, PVP, and unreacted Ag precursors. Finally, it was dispersed in EG for seed growth. We used freshly prepared solutions prepared on the day of synthesis and introduced a continuous flow of Ar gas (250 SCM) above the reaction mixture during the synthesis. The concentration of Ag was analyzed using ICP-OES (Varian 720-ES).

3. Seed-mediated Growth of Nanowires

We followed our previous procedure of seed-mediated growth of nanocubes [26]. Typically, the mixture of 3 mL of EG and 100 μL of 60 mM HCl in EG was preheated at 160 °C for 10 min with stirring (350 rpm) in a 22 mL vial under Ar gas introduction. 1 mL of 1.6 M $AgNO_3$ in EG was quickly added to the preheated EG. After 2 min, 1 mL of 0.4 M (or 0.8 M) PVP in EG was added, and 100 μL of seed nanowires was added after another 3 min. 20 min after the injection of seed nanowires, Ar gas flow rate was reduced to 150 SCM, and, after another 10 min, Ar introduction was stopped and the vial was capped. After 10 min, the product was quenched in a water bath at room temperature. It was washed with acetone once and with water several times to remove EG, PVP, and unreacted Ag precursors. All experiments were conducted in a dark room atmosphere to minimize the effect of photoreduction of Ag precursors.

4. Instrumentation and Characterization

SEM images were taken using a field-emission scanning electron microscope (JEOL 6500F). To determine the average size of nanowires and nanocubes, at least 100 particles were analyzed by imaging software (Image J) from scanning electron microscopy (SEM) images. Based on the data, the standard deviation in the dimension of nanowires and nanocubes was calculated. The list of

Table 1. Seeds and products, and summary of their dimension

#	Sample name	HCl vol.	PVP vol.	Seed vol.	Diameter	Length	Aspect ratio
1	Seed	-	-	-	63.0±6.4 nm	8.0±3.3 μm	127
2	H0	-	1 mL (PVP 55k 0.4M)	100 μL	-	-	-
3	H25	25 μL			-	-	-
4	H50	50 μL			84.0±13.0 nm	4.1±1.3 μm	48.8
5	H100	100 μL			660±100 nm	31.8±13.0 μm	48.2
6	H150	150 μL			790±170 nm	38.0±16.0 μm	48.1
7	P55k04	100 μL	1 mL (PVP 55k 0.4M)	100 μL	660±100 nm	31.8±13.0 μm	48.2
8	P360k04		1 mL (PVP 360k 0.4M)		1.3±0.2 μm	10.5±4.5 μm	8.1
9	P55k08		1 mL (PVP 55k 0.8M)		390±34 nm		-
10	P360k08		1 mL (PVP 360k 0.8M)		404±15 nm		-
11	S100	100 μL	1 mL (PVP 55k 0.8M)	100 μL	390±34 nm		
12	S200			200 μL	794±120 nm	56.0±14.0 μm	70.5
13	S500			500 μL	1.6±0.2 μm	3.7±1.4 μm	2.3

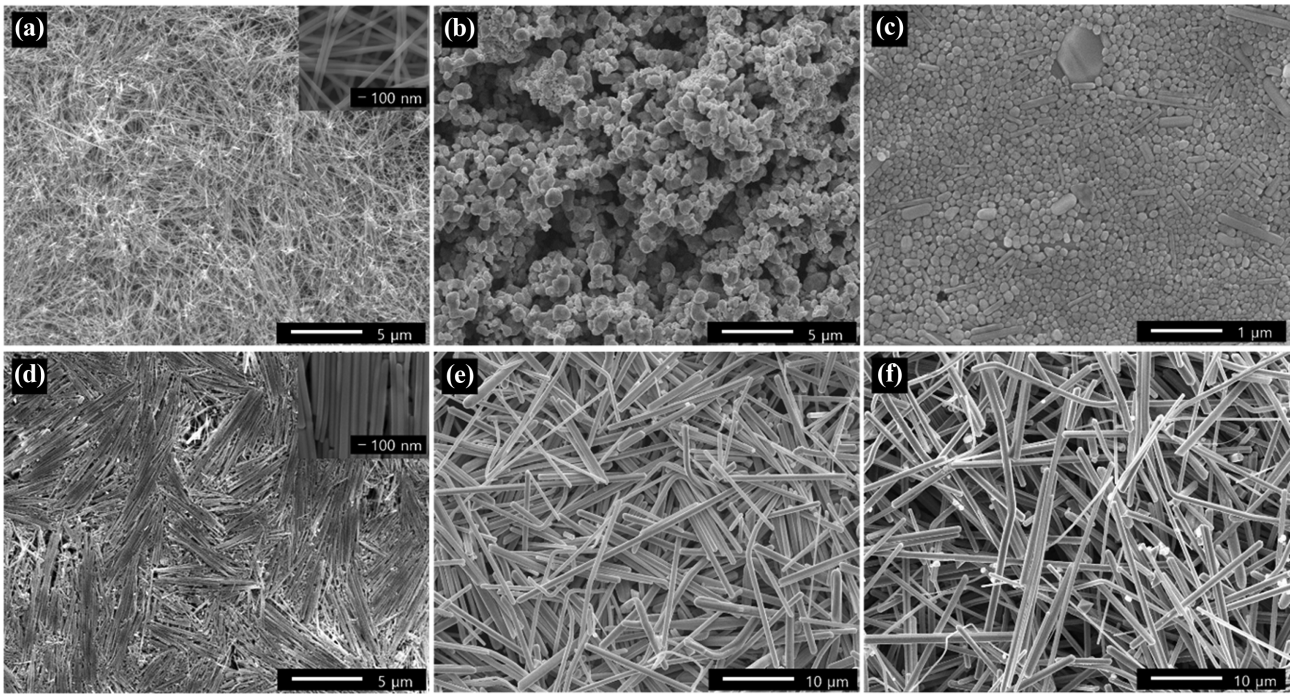


Fig. 1. SEM images of (a) seeds and (b-f) products obtained for a different amount of HCl solution added. (b) 0 μL, (c) 25 μL, (d) 50 μL, (e) 100 μL, and (f) 150 μL of HCl.

seed and products and summary of their dimensions are shown in Table 1.

RESULTS AND DISCUSSION

We synthesized seed Ag nanowires by polyol synthesis with $CuCl_2$ and a continuous flow of Ar gas to minimize the effect of oxygen [23,26]. Seed nanowires with an average diameter of 63.0±6.4 nm and an average length of 8.0±3.3 μm were successfully synthesized by the method (seed, Fig. 1(a)). Sufficient amount of batches of seed nanowires were collected in a large container and used for seed-mediated growth to minimize the effect of differences in seed quality from batch to batch. The concentration of Ag nanowires in the stock solution measured by ICP OES was 0.56 μg/mL. We used the seed-growth method that has been used for the growth of Ag nanocubes up to 3 μm without losing cubic shape [26].

We began the study regarding the effect of the amount of HCl solution (60 mM in EG) to explore an optimal condition for the growth of Ag nanowires by keeping the volume of $AgNO_3$, PVP, and seeds the same as summarized in Table 1. If HCl was not added, agglomerated irregular shape particles were observed (H0, Fig. 1(b)) because the formation of AgCl known to promote stabilization [19,25] and heterogeneous nucleation [20] is not possible due to the absence of Cl^- ion. For 25 and 50 μL of the HCl solution, severely truncated particles (H25, Fig. 1(c)) and nanowires that are slightly shorter and thinner than seeds were observed (H50, Fig. 1(d)), respectively. We speculate that those particles were formed by homogeneous nucleation due to insufficient HCl, evidenced by their size smaller than seeds and an enormous increase in the number of particles compared to that of seeds injected. For 100 (H100) and 150 μL (H150) of the HCl solution, nanowires much longer and thicker than seeds were obtained (Fig. 1(e)-(f)). It is expected that the seed-grown nanowires are successfully obtained by suppression of homogeneous nucleation by the increased amount of HCl. From the results, we conclude that 100 μL of HCl solution is sufficient for obtaining seed-grown nanowires, and thus the condition is used for further experiments.

Having established an optimal concentration of HCl, we turned to the study regarding the effect of PVP concentration and molecular weight. Two different molecular weight PVP, PVP 55k and PVP 360k, were used. For 1 mL of 0.4 M PVP 55k solution (P55k04), Ag nanowires with average diameter and length of 660±100 nm and 31.8±13 μm, respectively, were observed (Fig. 2(a)). If 1 mL of 0.4 M PVP 360k solution was used (P360k04), Ag micro rods were observed, and their diameter and length showed a large deviation (Fig. 2(b)). It has been reported that higher molecular weight PVP reduces the diameter of product nanowires due to stronger adsorption of higher molecular weight PVP to the Ag nanocrystal surface [39], opposite to the result shown here. In our case, at least three species, PVP 55k, Cu^{2+}, and Cl^-, were adsorbed on the surface of Ag during the synthesis of seeds, which may have affected the adsorption of higher molecular weight PVP in the seed-mediated growth. A further investigation into the cause of this phenomenon is ongoing. Interestingly, for 1 mL of 0.8 M PVP 55k (P55k04) and PVP 360k solution (P360k04), uniform Ag nanocubes with an edge length near 400 nm were observed, as shown in Fig. 2(c). We speculate that homogeneous nucleation was dominant because the nanowires were not able to grow when the PVP concentration was too high [40], and the reduction rate was increased by the higher concentration of PVP [16].

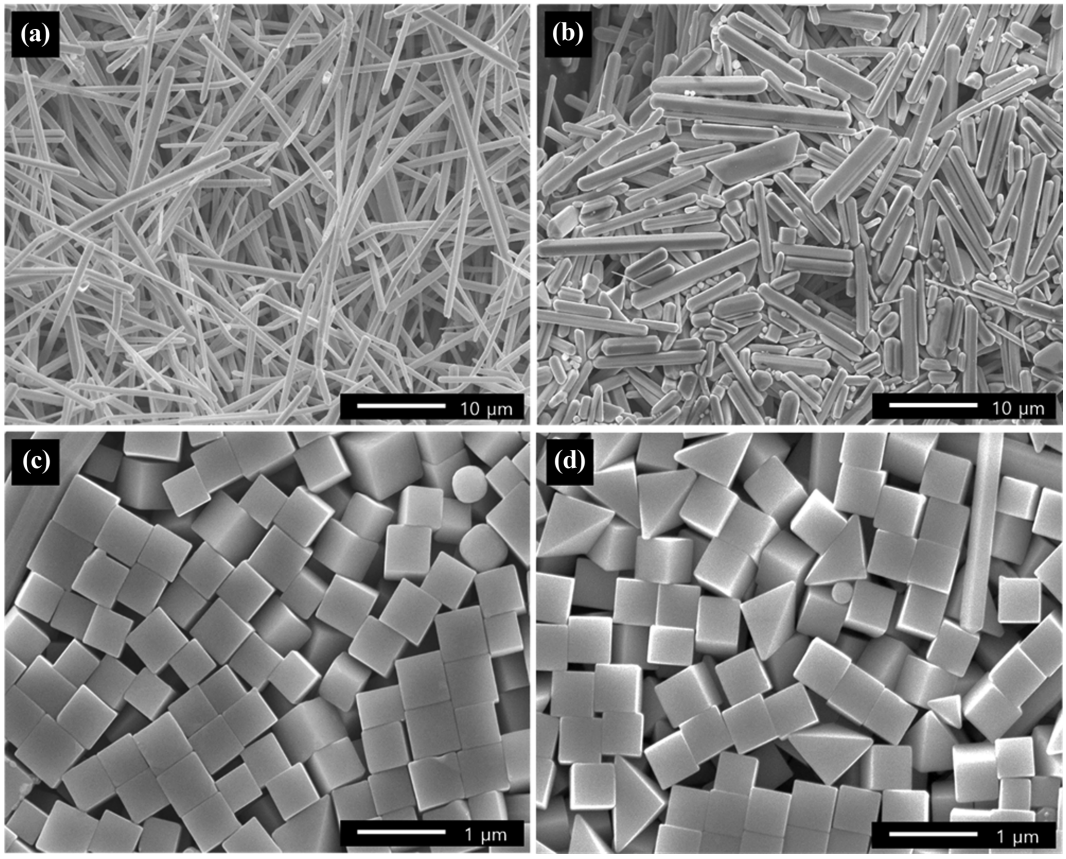


Fig. 2. SEM images of products for a different amount of PVP solution added. (a) 1 mL of 0.4 M PVP 55k, (b) 1 mL of 0.4 M PVP 360k, (c) 1 mL of 0.8 M PVP 55k, and (d) 1 mL of 0.8 M PVP 360k.

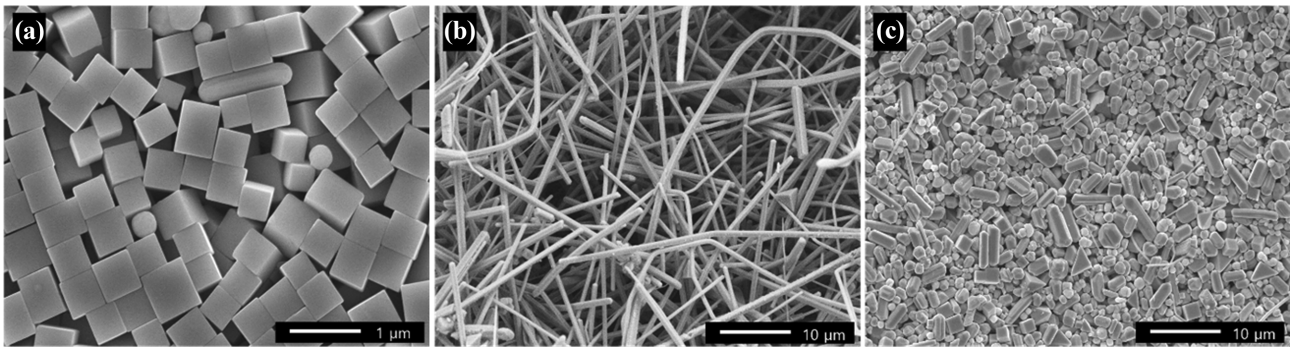


Fig. 3. SEM images of products for a different amount of seeds added. (a) 100 μL, (b) 200 μL, and (c) 500 μL.

Finally, the effect of the number of seeds was explored using the experimental condition resulting in nanocubes (P55k08). For 100 μL of seed solution (S100), nanocubes were observed as shown in Fig. 3(a), but if we increased the seed amount to 200 μL, grown nanowires were observed (S200, Fig. 3(b)). The average diameter and length of the observed nanowires were 794±120 nm and 56.0± 30.0 μm, respectively. We speculate that the increased total surface area by the increase in the number of seed nanowires was now sufficient for the consumption of the amount of Ag precursor, and thus seed-grown nanowires were obtained by the suppression of homogeneous nucleation. If we increased the number of seeds further to 500 μl, Ag particles of various shapes were observed together (S500, Fig. 3(c)). We speculate that the deficiency of PVP and Cl^- ions due to too much increase in the total surface area caused the large variety of shapes. It is also supported by the fact that the shape of the truncated particles shown in Fig. 3(c) is almost the same as the particles observed for the case with an absence (H0) or too low concentration of HCl (H25). Due to deficiency of HCl, homogeneous nucleation was dominant, and only some portion of seeds grew to cubes, bipyramids, and rods because of low concentration of HCl and PVP. Especially for multiply twinned seeds, if {100} facets of Ag nanowires were not sufficiently covered with

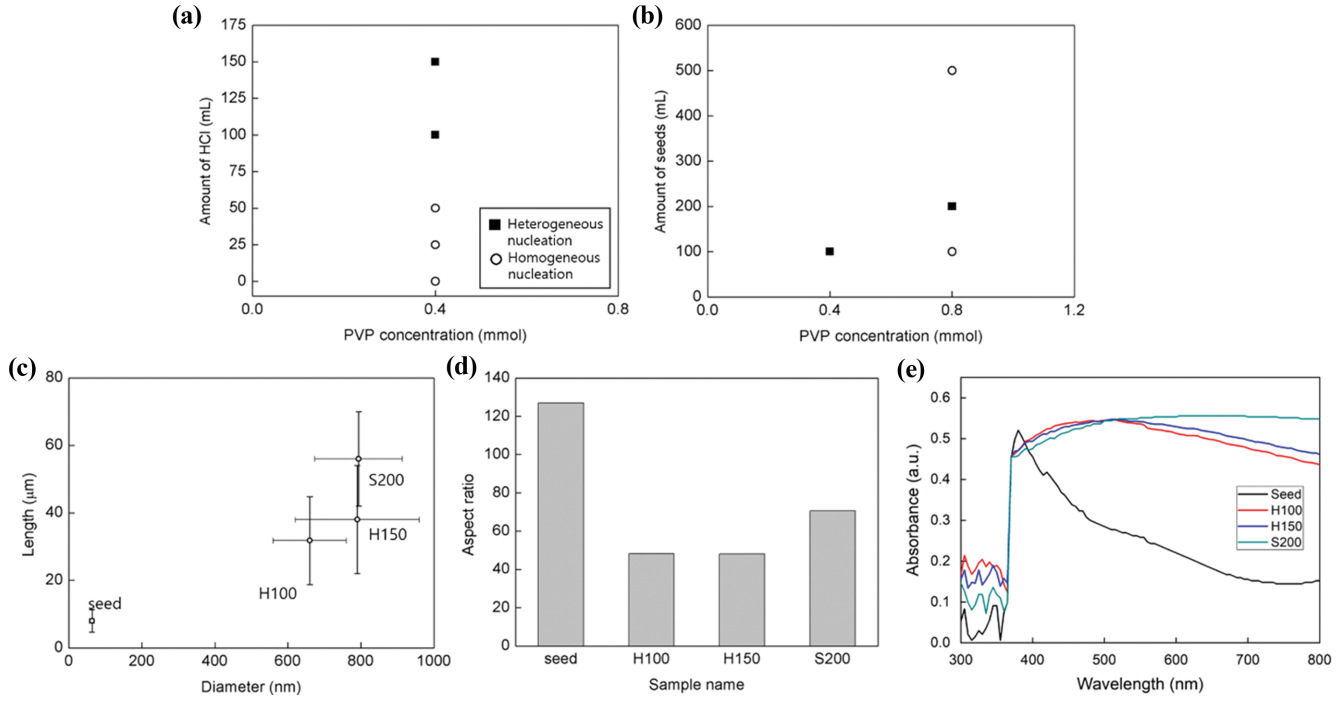


Fig. 4. Nucleation route determined by (a) amount of HCl added for 0.4 mmol PVP, and (b) amount of seeds added for 0.4 and 0.8 mmol PVP (Open circle: homogeneous nucleation, closed square: heterogeneous nucleation) (c) Summary of diameter and length, (d) aspect ratio, and (e) UV-vis absorption spectra of seed and seed-grown nanowires.

PVP, selective growth to {111} facets was not allowed, which caused the formation of rods [29].

We summarize the nucleation routes according to the concentration of PVP, HCl, and seeds in Fig. 4(a)-(b). The region for heterogeneous nucleation is clearly distinguished from homogeneous nucleation by a boundary of 100 μL HCl concentration in Fig. 4(a). But, regarding seed amount, heterogeneous nucleation is observed in the region between 100 and 500 mL of seed amount when PVP concentration is 0.8 mmol (Fig. 4(b)). We summarize the length and diameter of nanowires obtained by heterogeneous nucleation in Fig. 4(c). We note that seed-grown nanowires have a reduced aspect ratio than seed nanowires (Fig. 4(d)). The aspect ratio of seed-grown nanowires for H100, H150, and S200, is in the range between 48 and 70, which is smaller than that of seed, 127. Therefore, this method grows both the diameter and length of nanowires, especially the faster growth of diameter. In Fig. 4(e), UV-vis absorption spectra of seed and seed-grown nanowires are shown. Typical absorption spectra of Ag nanowires are observed for seed nanowires with the characteristic peak at 380 nm by the transverse plasmon mode [41], but a highly broad peak is obtained for seed-grown nanowires. The peak position of H150 is slightly red-shifted from that of H100, which may be due to 20% increase in length and thickness. H100 and H150 have almost the same aspect ratio of ~48, but the aspect ratio of S200, 70.5, is significantly larger that, due to 47% longer length but almost the same thickness. The spectrum for S200 is very broad and the absorbance across the whole visible wavelength range is almost uniform.

There has been considerable study on the lengthening of Ag nanowires to increase the electrical conductivity of Ag nanowire-based transparent electrodes for both one-pot synthesis [42-44] and seed-mediated growth [4,5]. But Wiley et al. reported that the thickening of Ag nanowires also helps improve the performance of the transparent electrode in case of low sheet resistance application [30]. And the size-controlled Ag nanowires are applicable to the study of the size-dependent properties of metals in the region between nano- to micro-meters [31-38]. Therefore, the synthesis method reported here not only provides a way to thicken nanowires but also opens new possibilities for the application of Ag particles in enhancement of electrical conductivity and mechanical strength.

Finally, if homogeneous nucleation occurs, various shape particles are obtained depending on the concentration of HCl, PVP, and seeds. For example, uniform nanocubes are observed for P360k08 (Fig. 5(a)). But if the same experiment is done without seed nanowires, a totally different product, a large number of non-uniform nanowires with irregular shape particles, is observed instead of the uniform nanocubes (Fig. 5(b)). Therefore, we can presume that seed nanowires play an important role in the formation of uniform nanocubes, though they do not play a role as seeds. It is known that twinned seeds have lower surface energy due to the significant lattice distortion and surface defects [18], and thus nanowires grown from multiply twinned seeds are more prone to be etched than newly created single crystalline seeds by homogeneous nucleation. Therefore, it is expected that nanowires sacrifice themselves to prevent newly created single crystalline seeds from etching, which causes the generation of uniform nanocubes. Recently, we synthesized nanocubes with similar size by seed-mediated growth of seed nanocubes [26]. The standard deviation of nanocubes obtained here, 15-34 nm, is similar to that of nanocubes shown in the pre-

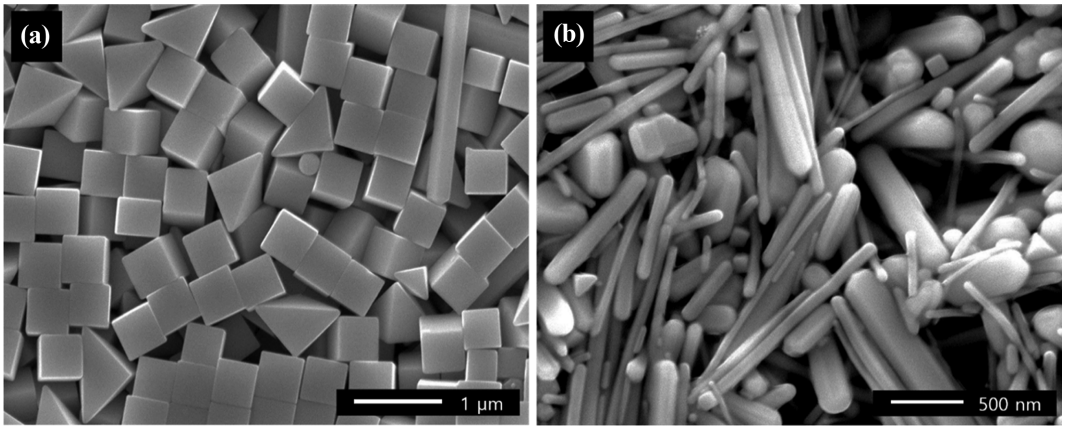


Fig. 5. The different final products, (a) uniform nanocubes and (b) mixture of non-uniform nanowires and irregular particles, obtained by the same experimental condition for homogeneous nucleation (P360k08) but with and without seeds, respectively.

vious report, 24-29 nm. So, this method can be used as another reliable method to synthesize uniform nanocubes.

CONCLUSIONS

We successfully synthesized seed-grown Ag nanowires by controlling the experimental parameters affecting nucleation routes. For 0.4 mmol PVP, the amount of HCl solution larger than 100 μL caused heterogeneous nucleation, while that smaller than 50 μL caused homogeneous nucleation. The condition for heterogeneous nucleation was quite sensitive to the PVP concentration. For example, heterogeneous nucleation was observed only for the seed amount higher than 100 mL and lower than 500 mL for 0.8 mmol PVP. With the optimized HCl, PVP, and seed concentration for heterogeneous nucleation, seed-grown nanowires were successfully obtained, and their size, the aspect ratio, and absorption spectra were analyzed. On the other hand, Ag particles of various shapes, including truncated particles, nanocubes, nanowires, and micro rods, were obtained with experimental conditions for homogeneous nucleation. This study provides an understanding of the factors affecting the nucleation routes and also provides a synthesis method for seed-grown Ag nanowires, applicable to the study of conductive electrodes and size-dependent properties of the metal particles.

ACKNOWLEDGEMENT

This research was supported by Kumoh National Institute of Technology (2017-104-158).

REFERENCES

1. Y. Xia, K. D. Gilroy, H.-C. Peng and X. Xia, *Angew. Chem. Int. Ed.*, **56**, 60 (2017).
2. K. D. Gilroy, A. Ruditskiy, H.-C. Peng, D. Qin and Y. Xia, *Chem. Rev.*, **116**, 10414 (2016).
3. V. K. LaMer and R. H. Dinegar, *J. Am. Chem. Soc.*, **72**, 4847 (1950).
4. J. H. Lee, P. Lee, D. Lee, S. S. Lee and S. H. Ko, *Cryst. Growth Des.*, **12**, 5598 (2012).
5. X.-Y. Zhang, J.-J. Xu, J.-Y. Wu, F. Shan, X.-D. Ma, Y.-Z. Chen and T. Zhang, *RSC Adv.*, **7**, 8 (2017).
6. B. Pietrobon, M. McEachran and V. Kitaev, *ACS Nano*, **3**, 21 (2009).
7. M. Mayer, L. Scarabelli, K. March, T. Altantzis, M. Tebbe, M. Kociak, S. Bals, F. J. García de Abajo, A. Fery and L. M. Liz-Marzán, *Nano Lett.*, **15**, 5427 (2015).
8. M. Luo, H. Huang, S.-I. Choi, C. Zhang, R. R. da Silva, H.-C. Peng, Z.-Y. Li, J. Liu, Z. He and Y. Xia, *ACS Nano*, **9**, 10523 (2015).
9. X.-Y. Zhang, X.-M. Xue, H.-L. Zhou, N. Zhao, F. Shan, D. Su, Y.-R. Liu and T. Zhang, *Nanoscale*, **10**, 15468 (2018).
10. M. Rycenga, C. M. Cobley, J. Zeng, W. Li, C. H. Moran, Q. Zhang, D. Qin and Y. Xia, *Chem. Rev.*, **111**, 3669 (2011).
11. W. Niu, L. Zhang and G. Xu, *Nanoscale*, **5**, 3172 (2013).
12. T. Zhang, Y.-J. Song, X.-Y. Zhang and J.-Y. Wu, *Sensors*, **14**, 5860 (2014).
13. X. Xia, J. Zeng, Q. Zhang, C. H. Moran and Y. Xia, *J. Phys. Chem. C*, **116**, 21647 (2012).
14. J. Zeng, Y. Zheng, M. Rycenga, T. Jao, Z. Y. Li, Q. Zhang, Y. Zhu and Y. Xia, *J. Am. Chem. Soc.*, **132**, 8552 (2010).
15. C. E. Hoppe, M. Lazzari, I. Pardinas-Blanco and A. Lopez-Quintela, *Langmuir*, **22**, 7027 (2006).
16. K. M. Koczkur, S. Mourdikoudis, L. Polavarapu and S. E. Skrabalak, *Dalton Trans.*, **44**, 17883 (2015).
17. Z. Chen, J. W. Chang, C. Balasanthiran, S. T. Milner and R. M. Rioux, *J. Am. Chem. Soc.*, **141**, 4328 (2019).
18. S. H. Im, Y. T. Lee, B. Wiley and Y. Xia, *Angew. Chem. Int. Ed.*, **44**, 2154 (2005).
19. B. J. Wiley, T. Herricks, Y. Sun and Y. Xia, *Nano Lett.*, **4**, 1733 (2004).
20. W. M. Schuette and W. E. Buhro, *ACS Nano*, **7**, 3844 (2013).
21. Z. Chen, T. Balankura, K. A. Fichthorn and R. M. Rioux, *ACS Nano*, **13**, 1849 (2019).
22. B. J. Wiley, Y. Sun and Y. Xia, *Langmuir*, **21**, 8077 (2005).
23. K. E. Korte, S. E. Skrabalak and Y. Xia, *J. Mater. Chem.*, **18**, 437 (2008).
24. Q. Zhang, W. Li, C. Moran, J. Zeng, J. Chen, L.-P. Wen and Y. Xia, *J. Am. Chem. Soc.*, **132**, 11372 (2010).
25. Z.-W. Lin, Y.-C. Tsao, M.-Y. Yang and M. H. Huang, *Chem. Eur. J.*, **22**, 2326 (2016).

26. S.-J. Jeon, S. Yazdi, R. Thevamaran and E. L. Thomas, *Cryst. Growth Des.*, **17**, 284 (2017).
27. X. Lin, S. Lin, Y. Liu, M. Gao, H. Zhao, B. Liu, W. Hasi and L. Wang, *Langmuir*, **34**, 6077 (2018).
28. C. Chen, L. Wang, H. Yu, G. Jiang, Q. Yang, J. Zhou, W. Xiang and J. Zhang, *Mater. Chem. Phys.*, **107**, 13 (2008).
29. M. Tsuji, X. Tang, M. Matsunaga, Y. Maeda and M. Watanabe, *Cryst. Growth Des.*, **10**, 5238 (2010).
30. S. M. Bergin, Y.-H. Chen, A. R. Rathmell, P. Charbonneau, Z.-Y. Li and B. J. Wiley, *Nanoscale*, **4**, 1996 (2012).
31. G. Y. Jing, H. L. Duan, X. M. Sun, Z. S. Zhang, J. Xu, Y. D. Li, J. X. Wang and D. P. Yu, *Phys. Rev. B*, **73**, 235409 (2006).
32. J. R. Greer and W. D. Nix, *Phys. Rev. B*: *Condens. Matter Mater. Phys.*, **73**, 1 (2006).
33. Y. Zhu, Q. Qin, F. Xu, F. Fan, Y. Ding, T. Zhang, B. J. Wiley and Z. L. Wang, *Phys. Rev. B*, **85**, 045443 (2012).
34. C. Peng, Y. Zhan and J. Lou, *Small*, **8**, 1889 (2012).
35. J. Wang, F. Sansoz, J. Huang, Y. Liu, S. Sun, Z. Zhang and S. X. Mao, *Nat. Commun.*, **4**, 1742 (2013).
36. M. D. Uchic, D. M. Dimiduk, J. N. Florando and W. D. Nix, *Science*, **305**, 986 (2004).
37. M. A. Mahmoud, D. O'Neil and M. A. El-Sayed, *Nano Lett.*, **14**, 743 (2014).
38. R. Thevamaran, O. Lawal, S. Yazdi, S.-J. Jeon, J.-H. Lee and E. L. Thomas, *Science*, **354**, 312 (2016).
39. R. R. Da Silva, M. Yang, S.-I. Choi, M. Chi, M. Luo, C. Zhang, Z.-Y. Li, P. H. C. Camargo, S. J. L. Ribeiro and Y. Xia, *ACS Nano*, **10**, 7892 (2016).
40. Y. Sun, B. Mayers, T. Herricks and Y. Xia, *Nano Lett.*, **3**, 955 (2003).
41. Y. Sun, B. Gates, B. Mayers and Y. Xia, *Nano Lett.*, **2**, 165 (2002).
42. H.-Y. Shi, B. Hu, X.-C. Yu, R.-L. Zhao, X.-F. Ren, S.-L. Liu, J.-W. Liu, M. Feng, A.-W. Xu and S.-H. Yu, *Adv. Funct. Mater.*, **20**, 958 (2010).
43. T. Araki, J. Jiu, M. Nogi, H. Koga, S. Nagao, T. Sugahara and K. Suganuma, *Nano Res.*, **7**, 236 (2014).
44. Y. Zhang, J. Guo, D. Xu, Y. Sun and F. Yan, *ACS Appl. Mater. Interfaces*, **9**, 25465 (2017).